

Parallel computing of elastic magnetic systems at the nanoscale

1st Artem V. Tomilo

Taras Shevchenko National University of Kyiv
Kyiv, Ukraine
tomilo.art.2018@knu.ua

3rd Kostiantyn V. Yershov

Leibniz Institute for Solid State
and Materials Research in Dresden
Dresden, Germany
k.yershov@ifw-dresden.de

2nd Oleksandr V. Pylypovsky

Helmholtz-Zentrum Dresden-Rossendorf e.V.
Dresden, Germany
o.pylypovsky@hzdr.de

4th Denis D. Sheka

Taras Shevchenko National University of Kyiv
Kyiv, Ukraine
sheka@knu.ua

Abstract—Intensive research in the area of nanoscaled physics opens new possibilities for the construction and fabrication of nanoscale devices. A numerical experiment is a powerful tool to analyze complex systems and flexibly check analytical predictions in addition to experimental validation. Therefore usage of parallel calculation is required to decrease the time of simulation.

Index Terms—Spin-lattice simulator, Landau-Lifshitz and Newtonian equation, magnetoelastic system, parallel computing, MPI, CUDA

I. INTRODUCTION

Soft magnetic materials open new possibilities in construction and fabrication of shapeable magnetoelectronics [1, 2], interactive human-machine interfaces [3, 4], and programmable magnetic materials [5, 6]. The shape of these materials determines their magnetic responses and can be controlled using external electric or magnetic fields. Moreover, remote control of the shape and 3D navigation of soft magnets stimulate intensive investigations in the area of micro-robotics [7, 8]. Recent progress in the synthesis of organic and molecule-based magnets opens new possibilities in the development of nanorobots devices, e.g., for organic spintronics [9]. In this context, the numerical experiment provides a third degree of freedom in addition to analytics and experiment to investigate fundamental and applied problems in the area of nanorobotics. In magnetism, the choice of specific technique is dependent on the materials and scales addressed by the given solver.

The micromagnetic simulation tools are widely used [10] for ferromagnetic materials with the main challenge to compute non-local magnetostatic interaction [11–14]. While flat films and bulk materials can be effectively described by finite difference integrators [15, 16], complex-shaped nanoparticles usually require finite elements techniques [12, 17]. In the same time, the micromagnetic approach can not properly handle singular magnetic textures, which require a local atomistic description [18, 19]. Purely atomistic simulations are represented by rapidly developing tools which can also address material-specific properties [20] and provide a potentially higher technical flexibility in an adjustment for specific problems [20–23], e.g., spin dynamics under influence of temperature, phase transitions and finite size phenomena.

Here, we describe a spin-lattice simulation suite SLasi for addressing not only rigid crystal lattices, but also elastic magnetic materials with exchange, Dzyaloshinskii–Moriya interaction (DMI) and dipolar coupling between spins, which is hardly accessible in conventional micromagnetic tools. The numerical solution of motion equations is accelerated using parallel computing with MPI and CUDA libraries. The correctness of calculations is verified by comparison with available analytical models.

II. MATHEMATICAL MODEL

Time evolution of magnetic moments in elastic lattice is described by a system of coupled Landau–Lifshitz–Gilbert

$$\frac{d\mathbf{m}_i}{dt} = -\gamma\mathbf{m}_i \times \mu_0\mathbf{H}_i^{\text{eff}} + \alpha\mathbf{m}_i \times \frac{d\mathbf{m}_i}{dt}, \quad (1a)$$

and overdamped Newton equations

$$\eta_i \frac{d\mathbf{r}_i}{dt} = -\frac{\partial\mathcal{H}}{\partial\mathbf{r}_i} + \mathbf{F}_i(\mathbf{r}_i, t), \quad i = \overline{1, N}. \quad (1b)$$

Here, $\mathbf{m}_i(t)$ is the unit vector of magnetic moment at the i -th lattice site with the radius-vector \mathbf{r}_i , $\gamma > 0$ is the gyromagnetic ratio, μ_0 is the magnetic permeability of vacuum, dimensionless parameter α characterizes the Gilbert relaxation, η_i is the coefficient of mechanical relaxation, $\mathbf{F}_i(\mathbf{r}_i, t)$ is the external force, and N is the total number of magnetic moments. The effective field $\mathbf{H}_i^{\text{eff}} = -(\mu_0 M_0)^{-1} \partial\mathcal{H} / \partial\mathbf{m}_i$ with M_0 being the dimensional length of magnetic moment includes the information about microscopic structure of the given magnetic material with the Hamiltonian \mathcal{H}

$$\begin{aligned} \frac{2\mathcal{H}}{S^2} = & \underbrace{-\sum_{i \neq j} J_{i,j} \mathbf{m}_i \cdot \mathbf{m}_j}_{\text{exchange}} - \underbrace{\sum_i \sum_{k=1}^3 K_i^k (\mathbf{m}_i \cdot \mathbf{e}_{i,k}^{\text{an}})^2}_{\text{anisotropy}} \\ & + \underbrace{\frac{\mu_0 M_0^2}{4\pi S^2} \sum_{i \neq j} \left[\frac{\mathbf{m}_i \cdot \mathbf{m}_j}{r_{ij}^3} - 3 \frac{(\mathbf{m}_i \cdot \mathbf{r}_{ij})(\mathbf{m}_j \cdot \mathbf{r}_{ij})}{r_{ij}^5} \right]}_{\text{magneto-dipolar interaction}} \\ & + \underbrace{\sum_{i \neq j} \mathbf{d}_{ij} \cdot [\mathbf{m}_i \times \mathbf{m}_j]}_{\text{DMI}} - \underbrace{\frac{2M_0\mu_0}{S^2} \sum_i \mathbf{m}_i \cdot \mathbf{H}_i^{\text{ext}}(t)}_{\text{External field}} + \mathcal{H}_{\text{el}}. \end{aligned} \quad (2)$$

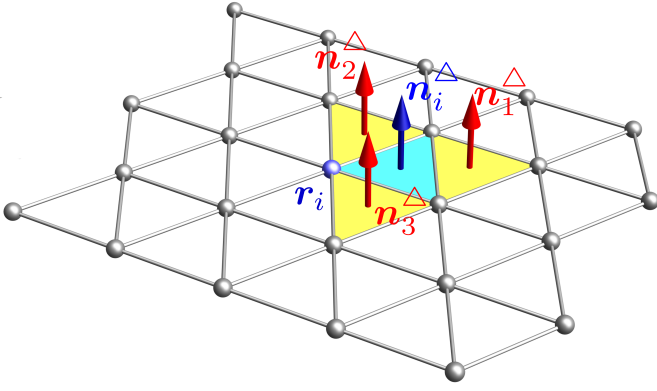


Fig. 1. Triangular lattice is implemented for 2D magnetoelastic systems. In the most general case, the triangle is a neighbor of 3 triangles with which it has a shared edge. The scalar product of the normal vectors for each pair of neighbor triangles is a separate term in the sum of the bending energy. If some triangle is missing, it is excluded from the calculation.

The exchange integral $J_{i,j}$ for the nearest neighbors takes positive and negative values for ferro- and antiferromagnetic coupling, respectively. Relativistic spin-orbit effects lead to an appearance of magnetic anisotropy within the lattice. Here, we consider the uniaxial single-ion anisotropy with coefficients K_i^k and axes $e_{i,k}^{\text{an}}$. The latter can be defined at each lattice site. The dipolar interaction between sites with radius-vector r_{ij} is essentially non-local and has the complexity $O(N^2)$ of calculation. The locally broken inversion symmetry of the lattice can be described by the Dzyaloshinskii–Moriya interaction with the DMI vector $d_{ij} = -d_{ji}$ for the neighboring spins. Different terms can be excluded from the consideration in specific problems. The last term, \mathcal{H}_{el} represents the elastic properties of the lattice:

$$\mathcal{H}_{\text{el}} = \frac{1}{2} \sum_{i \neq j} \lambda_i (|\mathbf{r}_j - \mathbf{r}_i| - a)^2 + \mathcal{H}_{\text{bend}}^{1,2D}. \quad (3)$$

The first term represents the stretching energy which controls the distance between the neighboring sites with equilibrium lattice constant a . The bending energy $\mathcal{H}_{\text{bend}}^{1,2D}$ takes different forms for chains arranged along space curves and two-dimensional lattices living at curved shells. In the one-dimensional case, it determines the change of angle between two neighboring bond vectors \mathbf{t}_i and \mathbf{t}_{i+1}

$$\mathcal{H}_{\text{bend}}^{1D} = \frac{1}{2} \sum_i \beta_i |\mathbf{t}_{i+1} - \mathbf{t}_i|^2, \quad \mathbf{t}_i = \frac{\mathbf{r}_{i,i+1}}{r_{i,i+1}} \quad (4)$$

with β_i being the bending coefficient and \mathbf{t}_i is a discrete tangential vector at i -th node [24]. We describe flexible magnetic shells using triangular lattice, see Fig. 1. The bending energy for the 2D system reads

$$\mathcal{H}_{\text{bend}}^{2D} = -\frac{1}{2} \sum_{i \neq j} \beta_i \mathbf{n}_i^\Delta \cdot \mathbf{n}_j^\Delta. \quad (5)$$

Here, \mathbf{n}_i^Δ is the normal vector to the triangle with vertex in r_i and j runs over nearest neighboring triangles.

III. SLASI ARCHITECTURE

SLaSi is a spin-lattice simulator that supports parallel computing using multiple cores of central processing units (CPU)

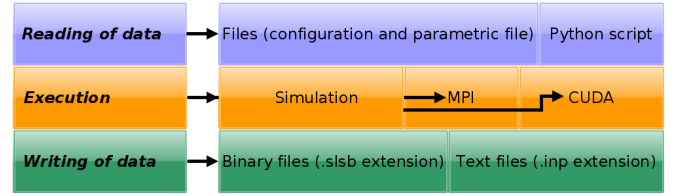


Fig. 2. SLaSi architecture: reading of simulation parameters, integration of (1) and saving output.

or graphical processing units (GPU). The program architecture consists of three levels (see Fig.2):

(i) *Data input* involves a general configuration file with setup of technical parameters for the numerical process and common material parameters for the whole sample; text table with site-specific parameters; Python script with functions calling for the evaluation of time- and coordinate-dependent parts of the Hamiltonian (2).

(ii) *Numerical process*. SLaSi is developed using C and is linked with Python modules to provide a way for the description of the initial magnetic texture and parameters as well as on-fly evaluation of magnetic fields and mechanical forces. For specific problems, calls of Python functions from the main code can slow down the calculation process. To provide a flexible user interface, the setup of the lattice parameters from a tab-separated file is available. A parallel computing is developed using MPI and CUDA libraries for CPU and GPU, respectively. The compilation of the software package is directed by CMake [25].

Evaluation of dynamical process (1) is performed by the Runge–Kutta–Fehlberg method of 4-5 order (RKF45) [26] with automatic step selection and the midpoint method (MP) [27] with the fixed step. RKF45 is suitable for use at CPU. The step control by comparison of the integration results by 4-th and 5-th order schemes with precision value allows a fulfillment of the required accuracy. Significantly different order of dynamics velocity in mechnical and magnetic subsystems requires tuning of the default precision for its increase. The precision for elastic system should be $10^5 \dots 10^{10}$ times higher than the precision for the rigid one. Automatic step selection using GPU requires to determine the maximal torque applied to magnetic moments within the given lattice, which slows down the CUDA processes itself. That's why we use MP for GPU computing with the pre-determined step values for the required precision.

(iii) *Output* can be performed using the internal binary SLSB or AVS UCD [28] formats. The SLSB is used to save disk space for the large-scale computations and allows to restart stopped numerical processes. AVS UCD is an open file format for the description of unstructured grids and is supported by open-source scientific visualization tools, e.g., ParaView [29].

IV. TESTING AND VERIFICATION

A conventional way to test micromagnetic solvers is to compare solutions of the so-called “standard problems” between different software packages [30, 31] and comparison with exact solutions if they are known. We start from the consideration of rigid systems and then consider flexible spin lattices.

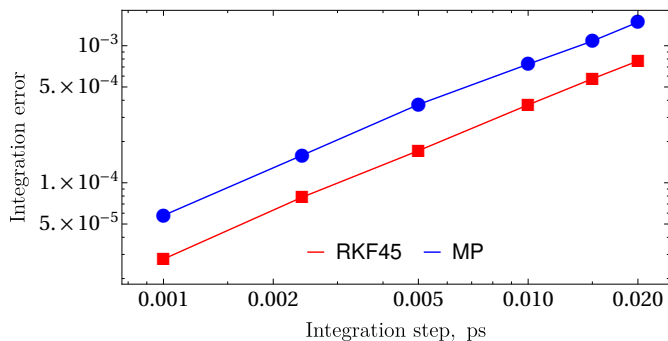


Fig. 3. Simulation error as a function of integration step for RKF45 and middle point methods.

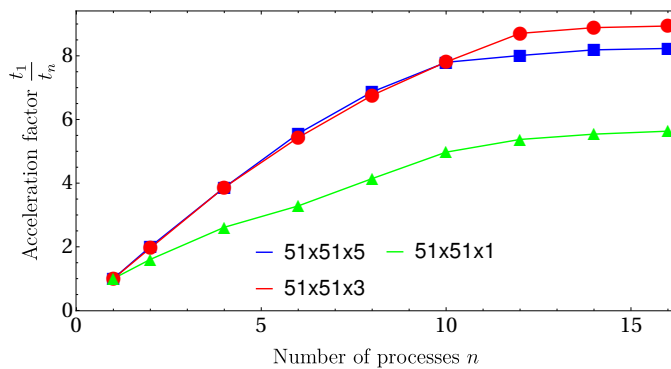


Fig. 4. Acceleration factor as a function of MPI launched processes number for physical systems that have different sizes.

A classical exactly solvable problem considers a macrospin relaxation under the action of the given effective field [32]. If the source of \mathbf{H}^{eff} is the uniform exchange and easy axis anisotropy, the dynamics of the magnetization reads

$$m_z(t) = \frac{m_{z0}}{\sqrt{m_{z0}^2 + (1 - m_{z0}^2)e^{-2\alpha\omega t}}}, \quad (6)$$

where m_{z0} is the initial vertical component of \mathbf{m} , and $\omega = \omega = KS/[(1+\alpha^2)\hbar]$ the resonance frequency of the given material. The final state in equilibrium is $m_z(t \rightarrow \infty) = 1$. Fig. 3 represents the error of the numerical process as a function of the selected integration step constant in time. The given plot shows the straight line on a log-log scale that means polynomial dependence of numerical error on the integration step. As expected, RKF45 shows a higher precision in comparison with MP, while the latter is twice faster in the absence of automatic step selection.

Interaction of magnetic dipoles in spin lattice macroscopically is usually treated in terms of magnetostatic interaction, while the anisotropic part of dipolar interaction is taken into account in magnetocrystalline anisotropy. The specific numerical implementation of this interaction is dependent on the scale of magnetic systems, addressed by the concrete solver. The $O(N^2)$ complexity allows an effective parallel computing of the dipolar/magnetostatic interactions. To test our MPI and CUDA implementation of the dipolar Hamiltonian we consider the relaxation of the Landau state in a square nanodot [33], see Fig. 4. The maximal performance depends on the nanodot size ($51 \times 51 \times (1, 3, 5)$ spins). The numerical experiment shows,

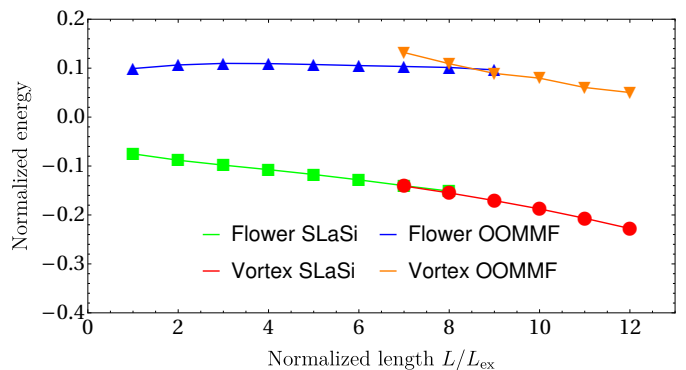


Fig. 5. Normalized energy $E/(\mu_0 M_s^2 V)$ as a function of the cube's edge size L/L_{ex} for vortex and flower ground states with M_s being the saturation magnetization, V is the volume, and L_{ex} is the exchange length. Micromagnetic simulator OOMMF and spin-lattice simulator SLaSi are used.

that the acceleration does not increase after 12 MPI processes due to Amdahl's law [34]. The same calculations using GPU show an acceleration 8.67 times for the size of the system $51 \times 51 \times 1$ in comparison with 1 CPU process.

To test the correctness of the dipolar interaction implementation, we solve the 3-rd standard μMAG problem [30] to compare the transition of isotropic ferromagnetic cube from vortex to flower states, see Fig. 5. These textures possess the different topologies and cannot be transformed into each other continuously. That's why we start the relaxation process from different initial states and compare their energies within the stability regions. SLaSi simulations are compared with their micromagnetic OOMMF framework [15]. The value of normalized length to switch between two ground states is slightly smaller from spin-lattice simulation in comparison with OOMMF. This is a result of the anisotropic part of the dipolar interaction which is not taken into account in OOMMF.

We consider a flexible ferromagnetic ring with an easy-tangential anisotropy as a prototypical system with a significant contribution of the elastic term \mathcal{H}_{el} . Such a quasi-one-dimensional system possesses two ground states depending on the magnetic and elastic properties as well as length [35]. The ground state of the long rigid closed chains corresponds to a circular shape and vortex circulation of magnetization. Otherwise, the so-called "onion" state is realized with the flat, ellipse-like chain shape and almost uniform magnetization in the plane of the chain [35]. Fig. 6 shows the comparison of analytics [35] (solid line) and SLaSi simulations (dots). The plot represents the component of the tangential vector as a function of the reduced arc length along the ring. Two flat regions correspond to the long sides of the elliptically deformed chain.

V. CONCLUSIONS

We develop and test the spin-lattice simulation software suite SLaSi for the investigation of rigid and elastic nanomagnets. CUDA and MPI libraries are used for speed-up of computations. SLaSi provides a convenient user interface that includes configuration files, Python scripting, and output files compatible with scientific visualization software.

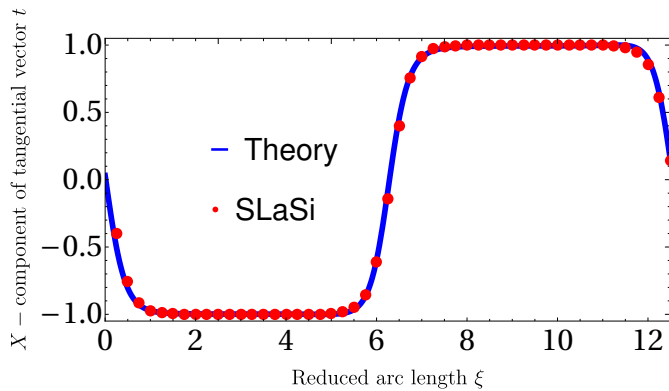


Fig. 6. X -component of tangential vector \mathbf{t} as a function of arc length coordinate ξ .

ACKNOWLEDGMENTS

Numerical experiments were performed using the clusters of Taras Shevchenko University of Kyiv [36] and Helmholtz-Zentrum Dresden-Rossendorf [37]. Artem V. Tomilo thanks Leibniz Institute for Solid State and Materials Research in Dresden for the internship on the project “Numerical study of flexomagnetic systems at nanoscale”.

REFERENCES

- [1] D. Makarov, M. Melzer, D. Karnaushenko, and O. G. Schmidt, “Shapeable magnetolectronics,” *Applied Physics Reviews*, vol. 3, no. 1, p. 011101, Mar. 2016. [Online]. Available: <http://dx.doi.org/10.1063/1.4938497>
- [2] P. Sheng, B. Wang, and R. Li, “Flexible magnetic thin films and devices,” *Journal of Semiconductors*, vol. 39, no. 1, p. 011006, Jan. 2018.
- [3] J. Wang, M.-F. Lin, S. Park, and P. S. Lee, “Deformable conductors for human-machine interface,” *Materials Today*, vol. 21, no. 5, pp. 508–526, Feb. 2018. [Online]. Available: <http://www.sciencedirect.com/science/article/pii/S136970211730559X>
- [4] W. Hu, G. Z. Lum, M. Mastrangeli, and M. Sitti, “Small-scale soft-bodied robot with multimodal locomotion,” *Nature*, vol. 554, no. 7690, pp. 81–85, Jan. 2018.
- [5] G. Z. Lum, Z. Ye, X. Dong, H. Marvi, O. Erin, W. Hu, and M. Sitti, “Shape-programmable magnetic soft matter,” *Proceedings of the National Academy of Sciences*, vol. 113, no. 41, pp. E6007–E6015, Sep. 2016.
- [6] Y. Kim, H. Yuk, R. Zhao, S. A. Chester, and X. Zhao, “Printing ferromagnetic domains for untethered fast-transforming soft materials,” *Nature*, vol. 558, no. 7709, pp. 274–279, Jun. 2018.
- [7] M. Medina-Sánchez, V. Magdanz, M. Guix, V. M. Fomin, and O. G. Schmidt, “Swimming microrobots: Soft, reconfigurable, and smart,” *Advanced Functional Materials*, vol. 28, no. 25, p. 1707228, Apr. 2018.
- [8] H. Ceylan, I. C. Yasa, O. Yasa, A. F. Tabak, J. Giltinan, and M. Sitti, “3D-printed biodegradable microswimmer for theranostic cargo delivery and release,” *ACS Nano*, vol. 13, no. 3, pp. 3353–3362, Feb. 2019.
- [9] P. Bujak, I. Kulszewicz-Bajer, M. Zagorska, V. Maurel, I. Wielgus, and A. Pron, “Polymers for electronics and spintronics,” *Chemical Society Reviews*, vol. 42, no. 23, p. 8895, 2013.
- [10] D. Kumar and A. O. Adeyeye, “Techniques in micromagnetic simulation and analysis,” *Journal of Physics D: Applied Physics*, vol. 50, no. 34, p. 343001, Jul. 2017.
- [11] D. Fredkin and T. Koehler, “Hybrid method for computing demagnetizing fields,” *IEEE Transactions on Magnetics*, vol. 26, no. 2, pp. 415–417, Mar. 1990.
- [12] T. Koehler and D. Fredkin, “Finite element methods for micromagnetics,” *IEEE Transactions on Magnetics*, vol. 28, no. 2, pp. 1239–1244, Mar. 1992.
- [13] C. Abert, L. Exl, G. Selke, A. Drews, and T. Schrefl, “Numerical methods for the stray-field calculation: A comparison of recently developed algorithms,” *Journal of Magnetism and Magnetic Materials*, vol. 326, pp. 176–185, Jan. 2013.
- [14] R. Hertel, S. Christophersen, and S. Börm, “Large-scale magnetostatic field calculation in finite element micromagnetics with H2-matrices,” *Journal of Magnetism and Magnetic Materials*, vol. 477, pp. 118–123, May 2019.
- [15] M. J. Donahue and D. G. Porter, “OOMMF user’s guide, version 1.0,” Interagency Report NISTIR 6376, Tech. Rep., 1999. [Online]. Available: <http://math.nist.gov/~MDonahue/pubs/abstracts.html#Donahue199909>
- [16] A. Vansteenkiste, J. Leliaert, M. Dvornik, M. Helten, F. Garcia-Sanchez, and B. Van Waeyenberge, “The design and verification of MuMax3,” *AIP Advances*, vol. 4, no. 10, p. 107133, Oct. 2014. [Online]. Available: <http://dx.doi.org/10.1063/1.4899186>
- [17] A. Kákay, E. Westphal, and R. Hertel, “Speedup of FEM micromagnetic simulations with graphical processing units,” *IEEE Transactions on Magnetics*, vol. 46, no. 6, pp. 2303–2306, Jun. 2010. [Online]. Available: <http://dx.doi.org/10.1109/TMAG.2010.2048016>
- [18] C. Andreas, S. Gliga, and R. Hertel, “Numerical micromagnetism of strong inhomogeneities,” *Journal of Magnetism and Magnetic Materials*, vol. 362, pp. 7–13, Aug. 2014. [Online]. Available: <http://dx.doi.org/10.1016/j.jmmm.2014.02.097>
- [19] C. Andreas, A. Kákay, and R. Hertel, “Multiscale and multimodel simulation of Bloch-point dynamics,” *Physical Review B*, vol. 89, p. 134403, Apr. 2014. [Online]. Available: <http://link.aps.org/doi/10.1103/PhysRevB.89.134403>
- [20] O. Eriksson, A. Bergman, L. Bergqvist, and J. Hellsvik, *Atomistic Spin Dynamics*. Oxford, United Kingdom: Oxford University Press, May 2017.
- [21] R. F. L. Evans, W. J. Fan, P. Chureemart, T. A. Ostler, M. O. A. Ellis, and R. W. Chantrell, “Atomistic spin model simulations of magnetic nanomaterials,” *Journal of Physics: Condensed Matter*, vol. 26, no. 10, p. 103202, Feb. 2014.
- [22] R. F. L. Evans, “Atomistic spin dynamics,” in *Handbook of Materials Modeling*. Springer International Publishing, 2018, pp. 1–23.
- [23] G. P. Müller, M. Hoffmann, C. Dißelkamp, D. Schürhoff, S. Mavros, M. Sallermann, N. S. Kiselev, H. Jónsson, and S. Blügel, “Spirit: Multifunctional framework for atomistic spin simulations,” *Physical Review B*, vol. 99, p. 224414, Jun. 2019. [Online]. Available: <https://link.aps.org/doi/10.1103/PhysRevB.99.224414>
- [24] S. Hu, M. Lundgren, and A. J. Niemi, “Discrete Frenet frame, inflection point solitons, and curve visualization with applications to folded proteins,” *Physical Review E*, vol. 83, no. 6, p. 061908, Jun. 2011.
- [25] “Official website of CMake.” [Online]. Available: <https://cmake.org/>
- [26] T. Ritschel, *Numerical Methods For Solution of Differential Equations*. Technical University of Denmark, 2013.
- [27] J. R. Chasnov, *Numerical Methods*. The Hong Kong University of Science and Technology, 2012.
- [28] “Description of AVS-UCD format.” [Online]. Available: http://www.hnware.de/rismo/dokumente/anwenderdoku/formate/avs_ucd.html
- [29] “Official website of ParaView.” [Online]. Available: <https://www.paraview.org/>
- [30] “μMAG – Micromagnetic Modeling Activity Group.” [Online]. Available: <https://www.ctcms.nist.gov/~rdm/mumag.org.html>
- [31] D. Cortés-Ortuño, M. Beg, V. Nehruji, L. Breth, R. Pepper, T. Kluyver, G. Downing, T. Hesjedal, P. Hatton, T. Lancaster, R. Hertel, O. Hovorka, and H. Fangohr, “Proposal for a micromagnetic standard problem for materials with Dzyaloshinskii–Moriya interaction,” *New Journal of Physics*, vol. 20, no. 11, p. 113015, Nov. 2018.
- [32] J. Coey, *Magnetism and Magnetic Materials*. Cambridge University Press, 2009.
- [33] S. E. Stevenson, C. Moutafis, G. Heldt, R. V. Chopdekar, C. Quitmann, L. J. Heyderman, and J. Raabe, “Dynamic stabilization of nonequilibrium domain configurations in magnetic squares with high amplitude excitations,” *Phys. Rev. B* 87, 054423, 2013.
- [34] J. Gustafson, *Encyclopedia of Parallel Computing*. Springer, 2011.
- [35] Y. Gaididei, K. V. Yershov, D. D. Sheka, V. P. Kravchuk, and A. Saxena, “Magnetization-induced shape transformations in flexible ferromagnetic rings,” *Physical Review B*, vol. 99, p. 014404, Jan. 2019. [Online]. Available: <https://link.aps.org/doi/10.1103/PhysRevB.99.014404>
- [36] “High-performance computing cluster of Taras Shevchenko National University of Kyiv.” [Online]. Available: <http://cluster.univ.kiev.ua/eng/>
- [37] “High Performance Computing at Helmholtz-Zentrum Dresden-Rossendorf.” [Online]. Available: <http://www.hzdr.de>